

THE EFFECT OF GROUND ICE MIGRATION ON THE MARTIAN PALEO-CO₂ BUDGET. E. David¹, O. Aharonson^{1,2}, E. Vos¹ and F. Forget³, ¹Weizmann Institute of Science, Rehovot, Israel (elad.david@weizmann.ac.il), ²Planetary Science Institute, Tucson, Arizona, ³Laboratoire de Météorologie Dynamique, Jussieu, Paris, France.

Introduction: CO₂ is a predominant constituent of the Martian climate system, and the response of the CO₂ cycle to the evolving orbit has been studied extensively [1][2]. However, a key factor that has yet to be thoroughly explored is the associated migration of the near-surface ground water ice in mid- to high latitudes, currently residing poleward of latitude ~45° [3][4]. Ground ice has been found by Haberle et al. [5] to affect the CO₂ cycle by increasing the thermal conductivity of the soil, while the geographic distribution of ground ice is believed to have varied significantly in the past as a function of the changing orbital parameters, namely eccentricity (e), longitude of perihelion (L_p) and obliquity (ϵ) [6][7].

In this work, we provide a systematic analysis of the effect of orbitally-forced redistribution of ground ice on the seasonal/secular CO₂ budget. We use a numeric model [8] to derive the equilibrium depth of the ice table at different orbital conditions and use the results as a boundary condition in the LMD-GCM [9]. We analyze the effect of changing ground ice distribution on the seasonal CO₂ accumulation at a given obliquity and outline how seasonal accumulation changes as a function of obliquity for end-member scenarios of static and equilibrium ground ice. These results illuminate a non-negligible aspect of the interplay between volatiles in the Martian climate system and are therefore of interest to the full reconstruction of the paleoclimate.

Methods & Results: We use the Global Climate Model developed by the Laboratoire de Météorologie Dynamique, CNRS, Paris (LMD-GCM) [9] in order to simulate the paleoclimate with different initial conditions of choice, focusing on orbital parameters and ground ice distributions. The model operates on a three-dimensional 64 x 64 x 29 grid (resolution of 2.8125° latitude and 5.6250° longitude) and calculates the temporal evolution of variables such as temperature, atmospheric pressure, and various tracers.

To obtain equilibrium ground ice distributions, we use a one-dimensional numeric model developed by Schorghofer & Aharonson [8] which calculates the depth of an ice table at ice-vapor equilibrium under a dry regolith layer for different orbital parameters. Mean annual daytime surface vapor pressure, a critical parameter for the ground ice model, is derived from GCM simulations (spin up time of 15 Mars-years). Ice table depths are subsequently adapted for the GCM subsurface scheme consisting of 18 grid points with

exponentially growing depth from 0.14 mm to 18 m. GCM ground ice is represented in terms of thermal inertia ($I = \sqrt{k\rho c_p}$) with the relation between pore fill fraction and thermal inertia following previous formulation [8]. Pore space ($\Phi = 0.4$) is assumed to be completely filled with ice under the ice table.

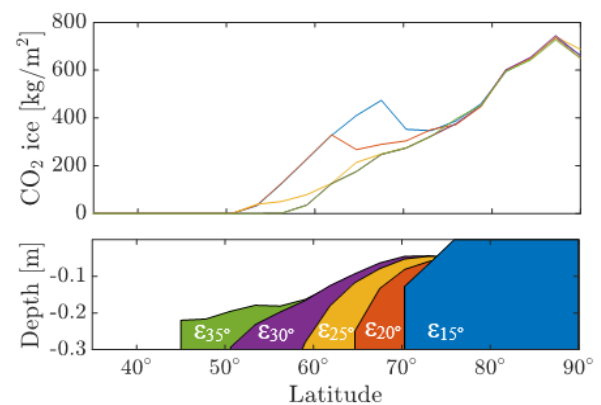


Figure 1: Northern hemisphere zonal mean CO₂ ice areal density (upper plot; $L_s = 320^\circ$; $\epsilon = 25^\circ$, $L_p = 270^\circ$, $e = 0.08$; simulation year 5) for selected ground ice distributions (lower plot; white \equiv no ice, color \equiv pores filled with ice).

Figure 1 shows the zonal mean CO₂ ice areal density at the northern hemisphere when the seasonal cap is at maximal extent ($L_s = 320^\circ$), obtained by GCM for a given set of orbital parameters ($\epsilon = 25^\circ$, $L_p = 270^\circ$ and $e = 0.08$) and various ground ice distributions (similar results were obtained for the southern hemisphere, not shown). Ground ice distributions are denoted by the obliquity with which each distribution is in equilibrium (e.g., ϵ_{15° denotes equilibrium ground ice at obliquity of 15°; with increasing obliquity lower latitudes receive less insolation, hence ground ice migrates equatorward). Notice that ground ice is treated here as a free variable, and obliquity remains 25° regardless of ground ice distribution. As ground ice extends equatorward (ϵ_{15° to ϵ_{35°), CO₂ ice accumulation steadily decreases. For the low obliquity distributions (ϵ_{15° and ϵ_{20°), the transition between icy and non-icy ground can clearly be noticed in the accumulation pattern as an abrupt rise. The decrease in accumulation can be intuitively understood: wherever ground ice is introduced, near-surface thermal conductivity increases, impeding CO₂ accumulation above it at autumn and winter. For obliquity of 25°,

mid-latitude ($<60^\circ$) accumulation is low enough that the extension of ground ice to these latitudes (from ε_{25° to ε_{30°) inhibits nearly any accumulation, and the seasonal cap margins recede poleward by $\sim 6^\circ$ latitude. Further equatorward extension of ground ice (from ε_{30° to ε_{35°) has little to no effect on CO_2 accumulation.

An expansion of these observations for additional obliquities is presented in Figure 2. Seasonal accumulation is represented as exchangeable mass of CO_2 (annual maximal – minimal CO_2 ice mass) per hemisphere. As expected, exchangeable mass decreases with extending ground ice. The "knee" in each curve is located at the distribution from which further ground ice extension no longer reduces accumulation, and it shifts equatorward with rising obliquity since the extent of the seasonal cap grows.

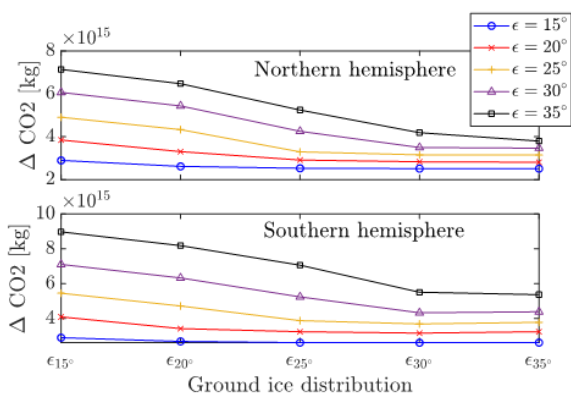


Figure 2: Exchangeable CO_2 mass per hemisphere as a function of ground ice distribution for selected obliquities ($L_p = 270^\circ$, $e = 0.08$).

From Figure 2 we can derive a function of exchangeable CO_2 mass as a function of obliquity (see Figure 3) for two hypothetical end-member scenarios: an "equilibrium scenario" where ground ice is in equilibrium distribution corresponding to the obliquity, and a "static scenario" where ground ice is in constant distribution regardless of obliquity (namely, ε_{25°).

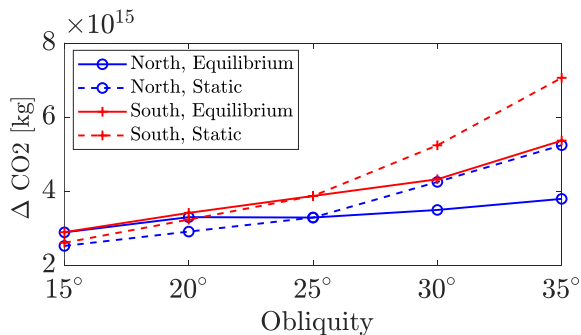


Figure 3: Exchangeable CO_2 budget as a function of obliquity ($L_p = 270^\circ$, $e = 0.08$) for northern and southern hemispheres at static and equilibrium ground ice scenarios.

Relative to the static scenario, in the equilibrium scenario exchangeable mass is higher at $\varepsilon \leq 25^\circ$ (ground ice retreats, allowing excess accumulation) and lower at $\varepsilon \geq 25^\circ$ (ground ice extends, retarding accumulation). The migration of ground ice to its equilibrium distribution reduces the rate of change of exchangeable mass with obliquity. Interestingly, at the northern hemisphere at $20^\circ \leq \varepsilon \leq 25^\circ$ ground ice migration completely offsets the insolation-forced rise in exchangeable mass resulting in a plateau in the curve, attesting to the significant effect ground ice migration has on seasonal accumulation.

Discussion: Our work emphasizes the notion that orbitally-forced ground ice redistribution is non-negligible and has potentially significant implications on the reconstruction of the Martian paleoclimate. Further work will develop our understanding of these effects on the seasonal/secular scale CO_2 budget, expand this analysis to other orbital parameters (*i.e.*, eccentricity and L_p) and interpolate to historic orbital parameter values to provide a fuller picture of the CO_2 budget's evolution. Finally, we must consider more realistic scenarios, such as non-equilibrium ground ice, ground ice in the presence of an equatorial humidity source, and others.

Acknowledgments: The authors wish to thank the Helen Kimmel Center for Planetary Sciences for support of this work and thank Norbert Schorghofer and Paul Hayne for helpful discussions.

References: [1] Toon, O. B., Pollack, J. B., Ward, W., Burns, J. A., & Bilski, K. (1980). *Icarus*, 44(3), 552-607. [2] Mischna, M. A., Richardson, M. I., Wilson, R. J., & McCleese, D. J. (2003). *Journal of Geophysical Research: Planets*, 108(E6). [3] Boynton, W. V., Feldman, W. C., Squyres, S. W., Prettyman, T. H., Brückner, J., Evans, L. G., & Shinohara, C. (2002). *Science*, 297(5578), 81-85. [4] Byrne, S., Dundas, C. M., Kennedy, M. R., Mellon, M. T., McEwen, A. S., Cull, S. C., & Seelos, F. P. (2009). *Science*, 325(5948), 1674-1676. [5] Haberle, R. M., Forget, F., Colaprete, A., Schaeffer, J., Boynton, W. V., Kelly, N. J., & Chamberlain, M. A. (2008). *Planetary and Space Science*, 56(2), 251-255. [6] Mellon, M.T., Jakosky, B.M. (1995). *Journal of Geophysical Research: Planets*, 100(E6), 11781-11799. [7] Chamberlain, M. A., & Boynton, W. V. (2007). *Journal of Geophysical Research: Planets*, 112(E6). [8] Schorghofer, N., Aharonson, O. (2005). *Journal of Geophysical Research: Planets*, 110(E5). [9] Forget, F., Hourdin, F., Fournier, R., Hourdin, C., Talagrand, O., Collins, M., Huot, J.P. (1999). *Journal of Geophysical Research: Planets*, 104(E10), 24155-24175.